Mutational Analysis of the P-Glycoprotein First Intracellular Loop and Flanking Transmembrane Domains†

Tony Kwan and Philippe Gros*

Department of Biochemistry, McGill University, 3655 Drummond Street, Montreal, Quebec H3G 1Y6, Canada

Received October 29, 1997

ABSTRACT: The role of individual intracellular (IC) loops linking transmembrane (TM) domains in P-glycoprotein (P-gp) function remains largely unknown. The high degree of sequence conservation of these regions in the P-gp family and other ABC transporters suggests an important role in a common mechanism of action of these proteins. To gain insight into this problem, we have randomly mutagenized a portion of TM2, the entire IC1 loop, TM3, the entire extracellular loop (EC2), and part of TM4, and analyzed the effect of such mutations on P-gp function. Random mutagenesis was carried out using *Taq* DNA polymerase and dITP under conditions of low polymerase fidelity, and the mutagenized segments were reintroduced in the full length *mdr3* cDNA by homologous recombination in the yeast *Saccharomyces cerevisiae* strain JPY201. The biological activity of mutant P-gp variants was analyzed in yeast by their ability to confer cellular resistance to the antifungal drug FK506 and the peptide ionophore valinomycin, and by their ability to complement the yeast *Ste6* gene and restore mating in a yeast strain bearing a null mutation [Raymond, M., et al. (1992) *Science 256*, 232−4] at this locus. The analysis of 782 independent yeast transformants allowed the identification of 49 independent mutants bearing single amino acid substitutions in the mutagenized segment resulting in an altered P-gp function. The mutants could be phenotypically classified into two major groups, those that resulted in partial or complete overall loss of function and those that seemed to affect substrate specificity. Several of the mutants affecting overall activity mapped in IC1; in particular we identified a segment of four consecutive mutation sensitive residues (TRLT, positions 169−172) with such a phenotype. On the other hand, we identified a cluster of mutants affecting substrate specificity within the short EC2 segment and in the adjacent portion of the neighboring TM4 domain. Expression and partial purification of a representative subset of these mutants showed that in all but two cases, loss of function was associated with loss of drug-induced ATPase activity of P-gp. Therefore, it appears that TM domains, IC and EC loops, are structurally and functionally tightly coupled in the process of drug stimulatable ATPase characteristic of P-gp.

A major limitation to the successful chemotherapeutic treatment of human tumors is the appearance of multidrug resistance (MDR). MDR in certain tumors in vivo and most cultured cell lines in vitro is characterized by cross-resistance to structurally and functionally dissimilar compounds and is associated with the overexpression of P-glycoprotein (P-gp), that functions as an energy-dependent efflux pump to reduce intracellular drug accumulation (*2*). P-gps are encoded by a small family of closely related genes with two members in humans (*MDR1* and *MDR2*) and three members in mouse (*mdr1*, *mdr2*, and *mdr3*). P-gps have been functionally classified into Class I (human MDR1, mouse Mdr1/Mdr3) and Class II molecules (human MDR2, mouse Mdr2) according to their ability to convey (Class I) or not the MDR phenotype (Class II) in transfection experiments (*2*, *3*). In normal tissues, P-gps function as lipid flippases (*4*) to translocate different types of phospholipids from the inner leaflet to the outer leaflet of the lipid bilayer in the canalicular membrane of hepatocytes (*5*) and possibly in other membranes (*6*). The mechanism of drug transport by Class I P-gps may be similar to the translocase mechanism of lipid transport demonstrated for these proteins in normal tissues. P-gps belong to the ABC (ATP-binding cassette) superfamily of transporters. Eukaryotic members of this family include the yeast *Saccharomyces cerevisiae* Ste6 protein that transports the *a*-factor mating pheromone (*7*), the Pfmdr-1 protein of *Plasmodium falciparum* which is associated with resistance to antimalarial drugs (*8*), the multidrug resistance related protein (MRP) initially found associated with drug resistance in lung cancer cells (*9*) and subsequently found to transport glutathione adducts (*10*), the transporter associated with antigen processing (TAP1/TAP2) which translocates peptides into the endoplasmic reticulum for association with MHC class I molecules (*11*−*14*), the cystic fibrosis transmembrane conductance regulator (CFTR) in which mutations cause cystic fibrosis in humans (*15*), and several others (*16*). Structural homology among ABC transporters translates into functional similarity, as P-gp (Mdr3) (*1*), MRP (*17*), and Pfmdr-1 (*18*, *19*) can all complement the yeast *STE6* gene and partially restore mating

† This work was supported by a grant (to P.G.) from the Medical Research Council (MRC) of Canada. T.K. was supported by a studentship from la Formation de Chercheurs et l'Aide à la Recherche (FCAR) and P.G. by a senior Scientist Award from the MRC.

* To whom all correspondence should be addressed: Tel: 514-398-7291, Fax: 514-398-2603, E-mail: gros@medcor.mcgill.ca.

S0006-2960(97)02680-9 CCC: $15.00
Published on Web 02/18/1998

in an otherwise sterile *ste6* mutant.

Secondary structure predictions suggest that P-gp is formed by two homologous halves, each encoding six transmembrane (TM) domains and a nucleotide binding (NB) site of the Walker type (*20*, *21*). The intracellular location of the two NB sites and the amino and carboxy termini of the protein has been verified by epitope mapping and protease digestion experiments (*22*, *23*). The exact number, orientation, and location of the 12 TM domains predicted by hydropathy profiling has been verified by a variety of methods including epitope tagging and immunofluorescence (*24*, *25*) and by insertion mutagenesis in a P-gp mutant lacking cysteines (*26*). Energy transfer experiments (*27*), epitope mapping studies of proteolytic P-gp fragments labeled with drug analogues (*28*), and genetic analyses of naturally occurring (*29*) or experimentally induced P-gp mutants with altered substrate specificity have shown that the TM domains are the major determinants for drug recognition and binding (*30*−*34*). On the other hand, direct biochemical characterization of the ATPase activity of intact P-gp and of inactive mutant variants bearing mutations in the predicted NB sites have indicated that ATP binding and hydrolysis at both sites is essential for P-gp mediated transport (*35*). A unique feature of the basal ATPase of P-gp (K_m = 1 mM and V_{max} = 0.3 to 2 μmol/min/mg protein) is that it can be further induced by both P-gp substrates and P-gp inhibitors, and a correlation between stimulation of ATPase activity and transport has been observed in certain substrate series (*36*). While certain compounds such as verapamil and vinblastine stimulate ATP hydrolysis, others like cyclosporin A do not stimulate P-gp ATPase activity but nevertheless inhibit stimulation by verapamil (*37*). These observations have led to the concept that substrate binding to TM domains of P-gp stimulates ATPase activity by the NB sites. While certain modulators that are transported by P-gp would mimic substrates and stimulate ATPase, others that are not transported would simply bind to TM domains and would uncouple the stimulatory signal to the NB sites. This signal transduction hypothesis is supported by the observations that (1) mutations near TM domains affect substrate specificity (*38*, *39*) by modulating drug binding (*40*), but also alter the pattern of drug-stimulatable ATPase activity (*41*); and (2) certain mutations in the NB sites affect the substrate specificity and drug resistance profile of the protein (*42*).

It has been proposed that intracellular (IC) loops linking individual TM domains may play an important role in transport in general, and possibly in signal transduction between the TM domains and the NB sites, in particular. This proposition is supported by both the high degree of sequence conservation in these regions in P-gp isoforms and in other ABC transporters, and by direct mutagenesis experiments. An important role for the predicted IC1 in this process has been suggested by the analysis of the G185V mutant of human MDR1 which emerged during in vitro selection for colchicine resistance (*39*). G185V maps in IC1, alters substrate specificity (increased colchicine resistance, reduced vinblastine resistance) by modulating drug binding to the protein (*40*), but also affects drug-induced ATPase activity of the protein (*41*, *43*). Furthermore, mutations at two additional glycine residues in this loop (G141, G187) also affect substrate specificity of MDR1 (*38*). In addition, the distribution of natural amino acid sequence polymorphisms in the rat TAP1/TAP2 proteins, that are associated with different peptide specificity of the transporter, cluster in the IC loops of the protein near the junction of TM domains (*44*). Finally, mutations at certain positions of IC loops of P-gp (*38*, *45*) and other ABC transporters (*46*, *47*) have been shown to affect protein stability and membrane targeting.

Altogether, these studies indicate that IC loops of P-gp play an important structural and functional role. In this study, we used random mutagenesis to systematically identify functionally important residues in the IC1 loop and neighboring segments of P-gp and carry out preliminary biochemical characterization of some of these P-gp mutants.

MATERIALS AND METHODS

mdr3 cDNA Modifications and Plasmid Constructions. A 1.7 kb *Sph* I-*Sma* I fragment of the N-terminal half of *mdr3* was cloned in the corresponding sites of bacteriophage vector M13mp19 and was used as a template for oligonucleotide mediated site-directed mutagenesis with a commercially available kit (Sculptor, Amersham). To facilitate subsequent cloning of the mutated cDNA fragments into an expression vector, *Nar* I and *Sac* II restriction sites flanking a cDNA segment overlapping part of TM2, the entire IC1 loop, and part of TM3 were introduced by mutagenesis using oligonucleotides [$^{5'}$GTGTATCTGGCGCCCAGCTGCC$^{3'}$] (*Nar* I site, nucleotide position 561) and [$^{5'}$CTTCCAGCCGCGGGTAAATC$^{3'}$] (*Sac* II site, nucleotide position 766). These mutations are silent and do not affect the amino acid sequence of the protein. The integrity of the mutated cDNA insert was verified by nucleotide sequencing using the dideoxy chain termination method of Sanger et al. (1977). A 318 bp cDNA fragment containing the *Nar* I/*Sac* II cassette was then excised using *Spl* I (position 477) and *Msc* I (position 795) and cloned into the full length *mdr3* cDNA present in plasmid vector pGEM-7Zf (pDR16) (*48*) to produce pGEM-7Zf/M3IC1. Finally, a 3.3 kb *Xba* I fragment (pst 70 to 3425) from pGEM-7Zf/M3IC1 was subcloned into the corresponding sites of the full-length *mdr3* cDNA contained in the yeast expression vector pVT-101U (pVTM3IC1). This vector allows expression and functional testing of P-gp activity in a yeast heterologous system that we have previously described (*49*). To express *mdr3* mutants in the *Pichia pastoris* system, a full length *mdr3* cDNA was cloned into the pHILD2 expression vector (Invitrogen) to generate pHILD2*mdr3*. Mutants Q128R, Q139H, F147L, E155L, T169I, T172P, G181R, A192T, W208G, L210I, and S224P were introduced into pHILD2*mdr3* by the direct replacement of an internal 1.6 kb *Afl* II/*Sma* I *mdr3* cDNA subfragment (pst 170 to 1764) by the corresponding mutated *mdr3* cDNA segment in pVTM3IC1. pHILD2 expression plasmids containing WT or mutant *mdr3* cDNAs were linearized with *Not* I and transformed into *P. pastoris* GS115 spheroplasts (Invitrogen) using a lithium chloride technique followed by plating onto MD medium (1.34% yeast nitrogen base, 4×10^{-5}% biotin, 1% dextrose). His$^+$ transformants were picked and streaked onto MM (1.34% yeast nitrogen base, 4×10^{-5}% biotin, 0.5% methanol) plates to identify clones showing successful homologous recombination events at the *AOX1* locus, and consequently displaying an impaired capacity to metabolize methanol (*m*ethanol *u*tilitizing slow

or mut^s). *His*$^+$ *mut*^{s} transformants were isolated and expanded in MD medium.

Random Mutagenesis of IC1 and Flanking Segments of Mouse Mdr3. To create a library of mutants within the 1st intracytoplasmic loop (IC1) and flanking segments of P-gp, we used random mutagenesis based on nucleotide misincorporation by polymerase chain reaction (PCR) under conditions of induced low polymerase fidelity (*50*). In this protocol, the concentration of one of the four nucleotide triphosphates is greatly reduced, resulting in *Thermophylus aquaticus (Taq)* polymerase pausing at positions corresponding to the nucleotide in limiting concentrations. Subsequently, *Taq* polymerase may at a low frequency randomly insert any dNTP at that position (or dITP when present), producing random mismatch mutations detectable in the full length PCR product of the reaction. Four separate reactions are set up, each with one nucleotide used at low concentrations. The concentration of $MgCl_2$ was varied between 0, 1, 2, 3, 4, and 5 mM to optimize the yield of PCR product for individual primer pairs used under limiting nucleotide concentrations. The amount of limiting dNTP to be used for random mutagenesis was optimized to yield single nucleotide substitutions in the final PCR product, in a series of pilot experiments (range between 14 μM and 20 μM). The mutation frequency was determined systematically after subcloning the PCR products into a poly-dT-tailed pBluescript vector (*51*), transforming the ligated plasmids into *E. coli*, and nucleotide sequencing of independent clones. Final conditions used for mutagenesis using oligonucleotides TM2F and TM4R were as follows: 10 ng of pVTM3IC1 DNA as template in a 50 μL reaction containing 50 ng each of TM2F [5′GTGCTCATAGTTGCCTACA3′, nucleotide position 512] and TM4R [5′CCAGCTCACAGTCCAAGAAC3′, nucleotide position 828] primers, 2 mM $MgCl_2$, 200 μM of three of the dNTPs, and 14 μM of the rate-limiting dNTP, 200 μM dITP (Pharmacia), and 1 unit of *Taq* DNA polymerase (Biocan, Montreal). The cycle program for the PCR reaction was 1 min at 94 °C, 1.5 min at 50 °C, and 2.5 min at 72 °C for a total of 25 cycles. Four reactions with each containing one of the four dNTPs in low concentration were independently set up, and the reactions were purified by phenol/chloroform extraction and ethanol precipitation and pooled to create the library. The pools of mutagenized segments were reintroduced back in the full-length *mdr3* cDNA by homologous recombination in yeast (*52*), according to the following protocol. Briefly, the pVTM3IC1 construct was digested with *Nar* I and *Sac* II to excise the 205 bp cassette overlapping the IC1 region. The shortened and linearized plasmid was dephosphorylated and purified by agarose gel electrophoresis. One microliter (corresponding to 500 ng of DNA) of each PCR reaction pool (for dATP, dCTP, dGTP, and dTTP) were added to approximately one hundred nanograms of linearized purified vector and cotransformed into the *S. cerevisiae* strain JPY201 (*MAT***a***ste6*Δ*ura3*) by the lithium acetate method followed by plating onto synthetic medium lacking uracil (SD-ura). Individual ura+ colonies were transferred into 100 μL of SD-ura in 96-well microtiter plates (Falcon), expanded in culture, and stored frozen in 30% glycerol at −80 °C.

Initial Screen for Functionally Impaired P-Glycoprotein. Screening of the library of mutants for the presence of P-gp variants with altered function was performed in yeast transformants by a growth inhibition assay that we have previously described (*53*) and that uses the antifungal drug and P-gp substrate, FK506. Each transformant (1 μL) was inoculated in a 96-well microtiter plate containing 100 μL of YPD medium supplemented with 50 μg/mL FK506 (OD_{595} at T_0 was approximately 0.05). Parallel control wells containing drug-free YPD medium were similarly inoculated with individual yeast transformants to determine normal growth for each transformant. Plates were grown with vigorous shaking for 20 h at 30 °C, and the optical density (A_{595}) was monitored in a standard ELISA plate reader. The growth of individual transformants in FK506 was measured as the relative growth compared to drug-free medium, and is expressed as a percentage.

Growth Inhibition and Quantitative Mass Mating Assay. Quantitation of the drug resistance phenotype expressed by individual P-gp mutants was determined by a growth inhibition assay in liquid medium for FK506 (50 μg/mL) and the peptide ionophore valinomycin (50 μg/mL). The ability of mutant P-gps to transport *a*-factor and to restore mating in a sterile *ste6* null mutant was performed as described previously by our group (*1*), with the following modifications. Briefly, JPY201 transformants were grown in NZM medium (0.35% NZ-amine, 0.75% yeast nitrogen base, 2% glucose) at 30 °C to midlogarithmic phase. Cultures were diluted to $A_{595} = 0.6$ in the same medium and grown for another 3 h at 30 °C. Next, 0.75 mL of transformant was mixed with 0.25 mL of the yeast tester stock DC17 (*MAT*α) grown to midlogarithmic phase ($A_{595} = 2$). A 0.25 mL aliquot of this mixture was then concentrated on a glass fiber filter which was then transferred to YPD agar and incubated 4 h at 30 °C to allow mating. Filters were then washed in 2 mL of minimal medium (0.68% yeast nitrogen base without amino acids, 2% glucose) with vigorous agitation to recover the cells. Cell suspensions were diluted appropriately (10^{-1} in minimal media, 10^{-5} in NZM media), and equal aliquots were plated in duplicate on minimal medium plates (number of JPY201 diploid cells formed by successful mating) and NZM plates (number of JPY201 haploid cells introduced in the assay). The ratio of the numbers of colonies obtained on each set of plates after incubation for 48 h at 30 °C was used to define the mating frequency.

Membrane Preparation. Yeast transformants were grown in SD-ura broth to late exponential phase ($A_{595} = 1.5-2.0$) and harvested. Cells were washed with lysis buffer (0.33 M sucrose, 5 mM EDTA, 1 mM EGTA, 2 mM DTT, 40 mM Tris pH 7.5) and resuspended in 250 μL of cold lysis buffer supplemented with protease inhibitors (10 μg/mL leupeptin, 10 μg/mL pepstatin A, 2.5 μg/mL chymostatin, 100 μM caproic acid, 1 mM PMSF). Cells were disrupted with 100 μL volume of acid-washed glass beads by vortexing six times with 1 min bursts at 30 s intervals (on ice). Unlysed cells were removed by centrifugation for 5 min at 12000*g* and total membranes were concentrated by ultracentrifugation for 30 min at 100000*g* at 4 °C (TLA100 rotor, Beckman tabletop ultracentrifuge). The final membrane pellet was resuspended in 25 μL of lysis buffer, and protein concentration was determined using a commercially available reagent (BioRad). For membrane isolation from *P. pastoris* transformants, all buffers were at 0 °C and supplemented with protease inhibitors (10 μg/mL leupeptin, 10 μg/mL

pepstatin A, 100 μM caproic acid, and 1 mM PMSF). For large scale preparations of *P. pastoris* membranes, 1 L of MD medium was inoculated with 5 mL of a culture in late-exponential phase and grown for 24 h and then transferred to 1 L MM medium for another 48 h to induce P-gp expression. Cells were centrifuged, resuspended in 40 mL of MM medium, and stored at −80 °C. Crude membranes were prepared from these stocks according to the protocol of Perlin et al. (*54*). Briefly, frozen cells were rapidly thawed at 30 °C and collected by centrifugation at 3000*g*, followed by resuspension in 40 mL of ice-cold homogenization buffer (0.33 M sucrose, 150 mM Tris pH 7.4, 1 mM EGTA, 1 mM EDTA, 2 mM DTT). Cells were passed twice through a French Press set at 20000 psi, adding fresh PMSF to the samples every 30 min. Large cell debris and unbroken cells were removed by centrifugation (14000*g*, 4 °C, 20 min), and crude membrane fractions were isolated from the supernatant by centrifugation (200000*g*, 4 °C, 90 min). Crude membrane pellets were resuspended in wash buffer (10 mM Tris pH 7.4, 1 mM EDTA, 10% (v/v) glycerol), homogenized 5× through a tight fitting glass homogenizer, and concentrated by centrifugation (200000*g*, 4 °C, 60 min). The pellets were resuspended in 5 mL of ice cold wash buffer using a 23 g needle and layered on top of a discontinuous sucrose gradient consisting of 16%, 31%, and 43% sucrose solutions containing 10 mM Tris pH 7.4 and 0.1 mM EDTA (TE), followed by centrifugation (53000*g*, 4 °C, 16 h). Membranes found at the various interfaces of the gradient were harvested, diluted to less than 0.25 M sucrose with TE, and recovered by centrifugation (200000*g*, 4 °C, 3 h). Membrane pellets were resuspended in mPIB buffer (0.33 M sucrose, 40 mM Tris pH 7.4, 1 mM EGTA, 1 mM EDTA, 2 mM DTT) and kept frozen at −80 °C.

P-gp Solubilization and Reconstitution in E. coli Lipids. P-gp was solubilized from the membrane fraction recovered at the interface of the 16% and 31% (w/v) sucrose solutions of the step gradient (16/31 membranes) using deoxycholate (DOC). Briefly, 16/31 membranes were solubilized at a final concentration of 0.5 mg/mL in solubilization buffer (0.33 M sucrose, 40 mM Tris pH 7.4, 1 mM EGTA, 1 mM EDTA, 1 mM DTT, 1.4% (w/v) DOC, 20% (v/v) glycerol, 0.4% (w/v) *E. coli* lipids, and protease inhibitors) by gentle vortexing at room temperature. Samples were centrifuged at 200000*g* for 1 h at 4 °C to remove insoluble material. *E. coli* lipids, dissolved in mPIB buffer, were added to the solubilized fraction to a final concentration of 1.4% (w/v). The samples were reconstituted by dialyzing against 200 volumes of dialysis buffer (40 mM Tris pH 7.4, 1 mM EGTA, 1 mM DTT) at 4 °C for 48 h. Reconstituted samples were aliquoted and stored at −80 °C.

ATPase assays. ATPase activity of the reconstituted fractions was estimated by measuring inorganic phosphate release by the colorimetric phosphate determination method of Van Veldhoven and Mannaerts (*55*). Basic ATPase cocktail consisted of 40 mM Tris pH 7.4, 10 mM ATP, 10 mM $MgCl_2$. EGTA (0.1 mM) and sodium azide (10 mM) were added to eliminate contaminating Ca^{2+}-ATPase and F_1-ATPase activity, respectively. Between 2 and 5 μg of reconstituted protein were added to 50 μL of cocktail and incubated at 37 °C in the linear range for ATP hydrolysis. P-gp substrates or modulators were added from fresh stocks in dimethyl sulfoxide.

SDS−PAGE Analysis and Immunoblotting. Crude membrane proteins were electrophoresed on a SDS-7.5% polyacrylamide gel and either stained with Coomassie brilliant blue R-250 or transferred onto a nitrocellulose membrane by electroblotting. The blots were blocked overnight at 4 °C in a solution containing 1% bovine serum albumin (Fraction V) in TBST (10 mM Tris pH 8.0, 150 mM NaCl, 0.05% Tween-20) followed by incubation for 1 h with the mouse anti-P-gp monoclonal antibody C219 (Centocor Corp., Philadelphia, PA) at a concentration of 1 μg/mL. Specific immune complexes were detected using a second goat anti-mouse antibody coupled to peroxidase used at a 1:10000 dilution and revealed by enhanced chemiluminescence (Amersham).

Immunofluorescence. Immunofluorescence analysis of yeast transformants expressing the mutant Mdr3 proteins was carried out according to a modification of a standard protocol (*17*). Transformants were grown overnight at 30 °C in 5 mL SD-ura media. Cells were fixed with 2.5 μL of 50% glutaraldehyde for 3 min. The cells were centrifuged and resuspended in 5 mL of 3.5% formaldehyde for 3 min, after which they were washed once each with PBS and SM buffer (1.2 M Sorbitol, 5 mM EDTA, 20 mM Tris, adjusted to pH 7.0). The cell wall was digested by resuspending the pellet in a mixture containing 1 mL SM buffer, 20 μL Zymolase (1 mg/mL), and 2 μL β-mercaptoethanol and incubating for 30 min at 37 °C. Spheroplasts were washed twice with SM buffer and then permeabilized as follows. To the pellet was added: 1 mL of ice cold methanol for 6 min and then 1 mL of ice cold acetone for 1 min, after which the suspension was immediately centrifuged for 2 min and the supernatant quickly decanted. The pellet was washed once with SM buffer, once in PBS containing BSA (fatty acid free, Boehringer-Manheim) at 1 mg/mL and finally resuspended in PBS/BSA (500 μL). Spheroplasts were incubated with a 1:200 dilution of rabbit anti-P-gp antiserum ES4 overnight at 4 °C on a rotating wheel. Excess primary antibody was washed extensively (10 times) with PBS/BSA before adding the secondary goat anti-rabbit antibody conjugated to Texas-red (used at a 1:2000 dilution) followed by incubation for 1 h at 20 °C. Cells were then washed extensively with PBS/BSA and the final pellet was resuspended in 100 μL of PBS. Immunofluorescence microscopy was performed using standard epifluorescence optics (Zeiss Axiophot).

RESULTS

Construction of Library of Mutants in the First Intracellular Loop Region of P-gp. Previous studies on naturally occurring (*39*, *40*) and experimentally induced (*38*, *45*) mutations in P-gp have suggested that intracellular (IC) loops in general, and IC1 in particular, may play an important role in substrate specificity (*38*−*40*, *45*), ATPase activity (*41*, *43*) and proper membrane targeting of P-gp (*38*). The aim of this study was to systematically identify residues of IC1 and neighboring segments that are important for P-gp function. For this, we applied a random mutagenesis approach to alter a mouse *mdr3* cDNA segment overlapping IC1 and flanking segments overlapping part of TM2, TM3, the short extracellular loop 2 (EC2) and a portion of TM4, followed by functional analysis of the P-gp mutants in a yeast expression system.

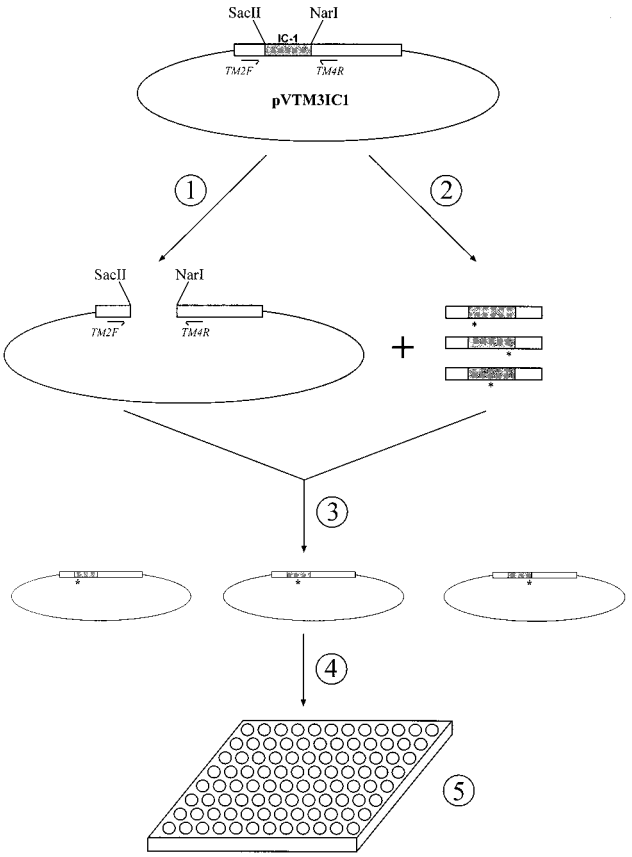

FIGURE 1: Protocol for the construction of a library of P-gp mutants. (1) The pVTM3IC1 plasmid containing the full length mouse *mdr3* cDNA is digested with *Sac* II and *Nar* I to remove the cassette to be mutagenized, (2) PCR random mutagenesis from pVTM3IC1 using oligonucleotide primers TM2F and TM4R, (3) homologous recombination in yeast by cotransformation of the gapped plasmid pVTM3IC1 with pools of mutagenized PCR products, (4) transfer of individual yeast transformants into 96-well plates containing growth medium lacking uracil, followed by freezing in 30% glycerol at −80 °C.

Our strategy for random mutagenesis was based on the polymerase chain reaction (PCR) under conditions of low polymerase fidelity, such that optimally each amino acid in this segment (delineated by two PCR primers) would be mutated to another residue (Figure 1). A first set of experiments was carried out to optimize the mutagenesis conditions for the *mdr3* DNA template, the oligonucleotide primers, and the batch of *Taq* DNA polymerase. Concentrations of $MgCl_2$ were varied between 1 and 5 mM, while the concentration of the limiting dNTP was varied between 14 and 20 μM. The efficacy of mutagenesis was estimated after subcloning the PCR fragments produced under each condition into a poly-dT-tailed plasmid (*51*), transformation into *E. coli*, and nucleotide sequencing of a sample of 20 clones. At optimal conditions ($MgCl_2$, 2mM; limiting dNTP, 14 μM), approximately 80% of the clones were found to bear mutations, with approximately 40% of single nucleotide substitutions. Under conditions where a single dNTP was used at limiting concentrations, we found that the total yield of PCR product was very low (possibly caused by low enzyme processivity). Inclusion of dITP in the reaction mixture increased the yield of PCR product, as it can substitute for both purines or pyrimidines allowing misincorporation and continued synthesis. PCR amplification of the dITP-containing strand results in the random incorporation of any nucleotide to replace inosine at that position. With these conditions, A to G and T to C transitions were predominantly observed when either dATP or dTTP were used in limiting concentrations. Similarly, when dGTP or dCTP were the limiting nucleotides, the most common substitutions seen were G to A and C to T. The frequency of these substitutions was 85% and approximately 15% were transversions (data not shown). Mutation frequencies observed in these pilot experiments were in good general agreement with those published by others (*50*) and were judged adequate for our analysis.

To maximize the efficiency of reintroducing the pool of mutagenized PCR fragments back into the full length *mdr3* cDNA, we used homologous recombination in yeast (*52*) between the PCR products and an expression vector containing the full length *mdr3* cDNA (Figure 1). The pVTM3IC1 (*ura-3*) construct was linearized with *Nar* I and *Sac* II to remove a 205 bp cDNA cassette that overlaps the mutagenized segment. Oligonucleotide primers used in the PCR reaction were designed to extend immediately upstream the *Nar* I and downstream the *Sac* II site by approximately 50 nucleotides, thereby providing sequence homology on either side of the gap between the pVTM3IC1 vector and the PCR fragments for homologous recombination by the yeast machinery (Figure 1). This gapped linearized vector was mixed with a pool of PCR-mutagenized *mdr3* fragments and cotransformed into the yeast strain *S. cerevisiae* JPY201 followed by selection of successful recombinants on SD-ura plates. The efficiency of homologous recombination by cotransformation was tested in pilot experiments. On average, 5×10^4 colonies per microgram of PCR product were obtained by this protocol, with a vector background (linearized and gapped pVTM3IC1) of less than 0.5%. Individual ura+ colonies were picked, grown in 100 μL ura- medium in 96-well microwell plates, and frozen in 30% glycerol. A total of 792 independent clones were isolated for study.

Initial Screen for P-gp Mutants with Altered Function. Expression of wild-type Mdr3 in yeast confers cellular resistance to the antifungal peptide macrolide FK506 (*53*), thereby providing an easy functional screen for P-gp mutants showing partial or total loss of function. A total of 792 yeast clones from the library were individually seeded either in control liquid medium and in medium containing FK506 at 50 μg/mL, and cellular growth was monitored by optical density over a period of 20 h. At that time, cell clones expressing wild-type Mdr3 had reached stationary phase in control and drug-free medium, while control pVT vector transformants showed complete growth in drug-free medium but no growth in FK506. Cellular resistance of individual mutants to FK506 was calculated as the relative growth of each clone in FK506 as compared to drug-free medium and was expressed as a percentage. This initial screen identified 109 clones that did not grow in FK506, while another 139 clones showed reduced growth with an intermediate phenotype (data not shown). This corresponds to 31% of the clones in the library harboring mutations deleterious to P-gp function. As our conditions for PCR mutagenesis give mutations in approximately 80% of the clones, this suggests that approximately 50% of mutations within the region defined by the PCR primers are either silent or induce changes that are neither detrimental to P-gp function or

Table 1: Summary of Mutations Identified[a]

TM2	IC1			TM3	EC2	TM4
Q128H	R138H	F159I	S176P	G187E	R206L	L210I
Q128R	Q139H	V161E	K177I	A192T	W208G	T211P
L134P	Q139P	H162R	N179S	F200L	K209E	V213A
A136V	Q139R	T169I	E180G	F204S		I214L
	Q145H	R170L	G181R			I214T
	F147L	L171P	G183D			S224P
	F148S	T172P	D184N			
	E155G	D174G				
	E155K	S176F				

[a] Summary of the mutations identified in the current screen together with their position within the predicted secondary structure of P-glycoprotein, with respect to the second (TM2), third (TM3), and fourth (TM4) predicted transmembrane domains together with the first intracellular (IC1) and second extracellular loop (EC2).

membrane targeting/processing. In fact, DNA sequence analysis of 10 random "mutant" clones showing wild-type levels of FK506 resistance identified single nucleotide substitutions in 8 out of 10 (data not shown).

The nucleotide sequence of the mutagenized cDNA segment delineated by primers TM2F and TM4R used for mutagenesis was determined for all plasmids giving rise to altered drug resistance phenotypes. Out of the 109 mutants that were functionally inactive for growth in FK506, we found only 5 with single amino acid substitutions within the mutagenized insert, while the remaining 104 contained either multiple amino acid substitutions, termination codons, or single base deletions or insertions. The latter two types are expected to produce truncated inactive proteins and were not studied further. Sequencing of the 139 mutants showing an intermediate drug resistance phenotype identified 44 clones harboring single amino acid substitutions, while the other 95 mutants carried multiple amino acid substitutions within the insert. The latter group of 95 mutants was not studied further, and we focused the remainder of our analysis on the group of 49 mutants (6.2% of the library) showing single amino acid substitutions leading to either a null or intermediate drug resistance phenotype. A listing of these mutants and their position within predicted secondary structural features of P-gp is shown in Table 1. The 106 amino acid segment of P-gp targeted for mutagenesis included a portion of TM2 (V121 to G137), IC1 (R138 to K185), TM3 (I186 to T205), EC2 (R206 to K209), and part of TM4 (L210 to G226). Mutations expressed as partial or complete loss of P-gp function in FK506 were found throughout the entire targeted region, at 36 of the 106 possible positions (34% of the residues). The frequency of the mutations were 30% for TM2 (3/10), 44% for IC1 (21/48), 20% for TM3 (4/20), 75% for EC2 (3/4), and 30% for TM4 (5/15). Therefore, IC1 (and EC2) were the most mutation sensitive portions of the segment tested.

Certain mutations were detected more than once in our screen; these included T169I (2×), L171P (2×), T172P (4×), E180G (2×), and G181R (2×). Sequencing identified the same nucleotide substitution in "independent" clones, suggesting that these did not emerge from independent mutagenic events but rather resulted from preferential amplification and/or cloning of a single mutagenic event in the PCR reaction. On the other hand, certain residues were found targeted more than once but with different amino acid substitutions each time; these included Q128 (H, R), Q139 (H, P, R), E155 (G, K), S176 (F, P), and I214 (L, T). The identification of independent mutations at these positions causing a partial or complete loss of function suggest that these residues play a critical role in either the structural organization or the mechanism of P-gp action and do not tolerate replacements without some loss of function.

Functional Analysis of Mdr3 Mutants Bearing Single Amino Acid Substitutions. Mutants bearing unique amino acid substitutions were analyzed further. First, the plasmids encoding these mutants were rescued and reintroduced into JPY201 cells to ascertain their activity and to eliminate possible contributions of extragenic mutations in the yeast genome to the phenotype. Second, we characterized additional aspects of P-gp function in these transformants. These included the capacity to confer resistance to another MDR drug, the peptide ionophore valinomycin (*56*), and the capacity to transport the yeast farnesylated peptide pheromone *a*-factor, by monitoring complementation of the endogenous *STE6* gene and restore mating in a sterile *ste6* null mutant (*1*). We tested a total of 42 independent mutants with unique single substitutions within the mutagenized segment.

Figure 3 shows histograms quantitating the degree of resistance (relative growth) to FK506 (50 μg/mL) and valinomycin (50 μg/mL) and the efficiency of mating expressed by yeast cells transformed either with a wild-type *mdr3* plasmid, the control pVT vector, or the individual mutants. Phenotypically, the mutants could be classified into three groups. The first group (group 1) included mutants showing a severely reduced function, with at least a 5-fold reduction in activity (less than 20% of wild-type) in at least two of the three assays. The second group (group 2) included mutants that showed an intermediate phenotype between group 1 and the wild-type protein in the same assays (between 20% and 70%). Finally, a third group (group 3) included mutants showing characteristics similar to the wild-type protein (between 70% and 100%) for all three assays. Figure 2A presents a diagrammatic summary of the position of the various groups of mutants onto the primary sequence of P-gp and the corresponding secondary features (TM domains, IC and EC loops). Group 1 comprised 17 mutants, including Q128R, L134P, F147L, F148S, F159I, V161E, H162R, T169I, R170L, L171P, T172P, G181R, G187E, W208G, K209E, I214L, and S224P. Group 1 mutants were distributed in the five topological domains tested (TM2, IC1, TM3, EC2, TM4); however, it is noticeable that four such mutations were identified at consecutive residues in IC1 (TRLT, Figure 2A), suggesting that these residues are particularly sensitive to alterations and are critical for function. Several of these group 1 mutants were also identified in a short 9 amino acid segment overlapping predicted EC2 and the adjacent portion of TM4. Group 2 comprised 19 mutants with intermediate phenotypes: Q128H, A136V, Q139H, Q139P, Q139R, E155G, E155K, S176P, K177I, E180G, G183D, D184N, A192T, F200L, F204S, R206L, L210I, T211P, and V213A; these were found throughout the mutagenized segment, with a cluster at the C-terminal portion of IC1. Finally, group 3 mutants included mutants R138H, Q145H, D174G, S176F, N179S, and I214T.

In addition to a reduction in overall activity, certain class 1 and class 2 mutants showed drastic alterations in substrate specificity. Such mutants showed near wild-type transport

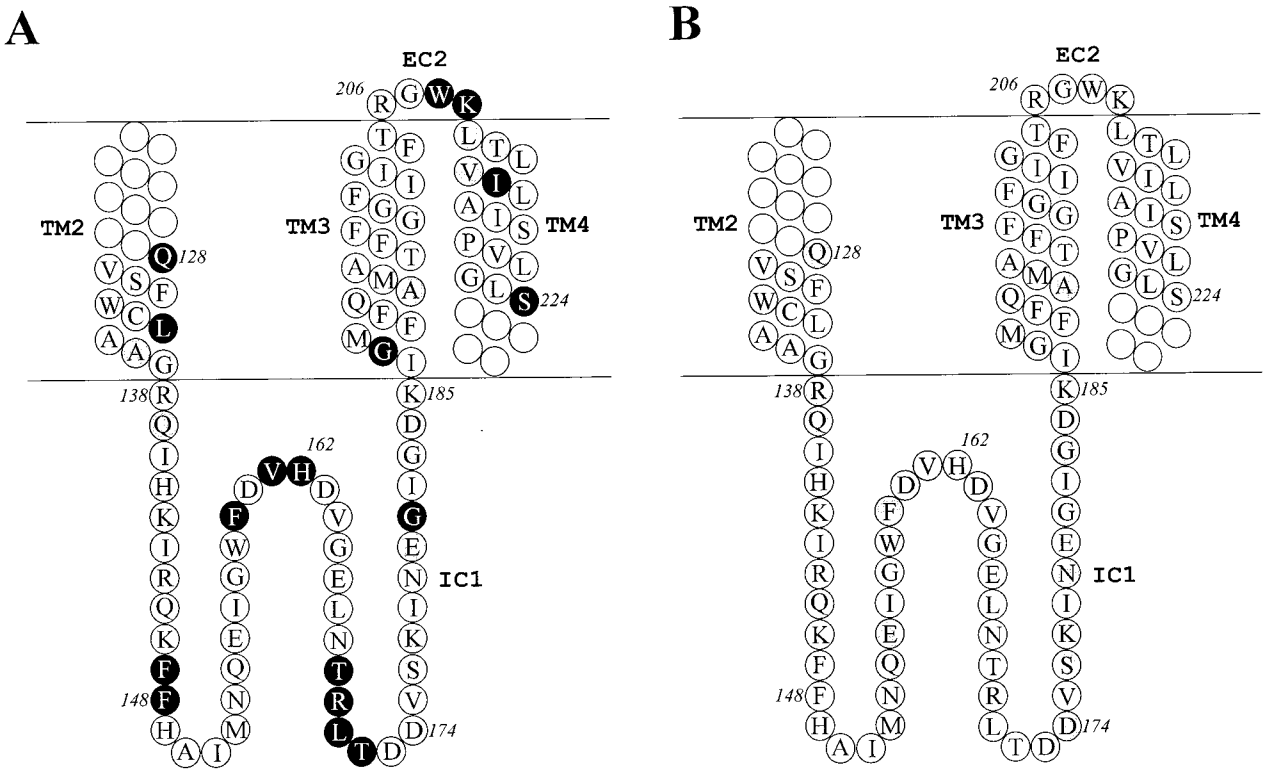

FIGURE 2: Position of individual mutants on the primary amino acid sequence and predicted secondary structure of P-gp. The position of the second (TM2), third (TM3), and fourth (TM4) transmembrane domains is shown together with the first intracellular (IC1) and second extracellular loop (EC2). (A) Positions of mutants with severe (dark shading) or intermediate (gray shading) reduction of activity toward two of the substrates tested (decrease in overall activity) are identified. (B) Residues shaded in gray denote mutations causing possible altered substrate specificity.

for one of the three substrates tested (FK506, valinomycin, *a*-factor), but severely reduced activity toward the other substrates tested. The most striking examples of such mutants include Q139H, Q139R, and F147L that showed wt activity for VAL (72−100%), severely reduced activity for FK506 (16−33%), and complete loss of function for mating (1−2%). Other mutants in this group including A192T and L210I retained robust activity against FK506 and VAL, but showed a severe reduction in mating activity. The position of mutants showing important deviations in substrate specificity from the wild-type protein have been positioned on the predicted structural features of the mutagenized segment in Figure 2B. Although mutants with this phenotype can be detected throughout the mutagenized domain, a cluster of such mutants is found in an 11 amino acid segment overlapping predicted EC2 and the immediately adjacent portions of TM3, but mostly TM4. Such mutants may be important for the architecture of a drug binding site in P-gp, or for TM helix packing to create such a site. Finally, we noted a group of mutants that showed mating activities superior (1.4× to 3.5×) to those observed with the wild-type Mdr3 protein. This group included Q145H (2.5×), D174G (3.5×), S176F (1.4×), N179S (2.2×), and I214T (2.6×). All these mutants mapped within the IC1 segment except I214T which was in TM4 (Figure 2B).

Together, these studies suggest two types of mutations in our library, those that seem to affect overall activity of the protein and those that seem to affect substrate specificity.

Detection of Mdr3 Mutants in S. cerevisiae. To verify that the various mutant Mdr3 proteins are properly synthesized, and targeted to the membrane in yeast, we carried out immunoblotting and immunofluorescence experiments on yeast transformants expressing individual mutants. This was particularly important in the case of Mdr3 mutants such as Q128R, L134P, V161E, R170L, L171P, G181R, G187E, and S224P that show complete loss of function in the three assays conducted. To determine if the mutant Mdr3 proteins were targeted to the membrane fraction of the cells, immunoblotting was carried out on equal amounts of crude membrane fractions (100000*g* pellet) from individual transformants, using the mouse anti-P-gp monoclonal antibody C219 (*23*) for detection. Results in Figure 4A identify the presence of an immunoreactive Mdr3 protein of approximate molecular mass 170kD in all transformants. The level of expression of these various proteins was similar among the clones, although not identical. Nevertheless, these results suggest that the various mutations did not drastically affect the processing of the various proteins, including their targeting to the membrane fraction of the cells. Immunofluorescence studies were conducted to assess possible effects of the mutations on the subcellular localization of the various proteins in intact cells. For this, cells were permeabilized with glutaraldehyde, and the various Mdr3 proteins were detected using the anti-P-gp antiserum ES-4 and a secondary sheep anti-rabbit antiserum coupled to fluorescein. Results from these experiments showed a very similar staining for all the cell clones analyzed which was similar to that seen in cells expressing wild-type Mdr3 and included both a ring-like staining at the periphery of the cells as well as a diffuse intracellular staining (data not shown). An example of this staining is shown in the insets of Figure 4B for cells expressing the wild-type Mdr3, control pVT plasmid trans-

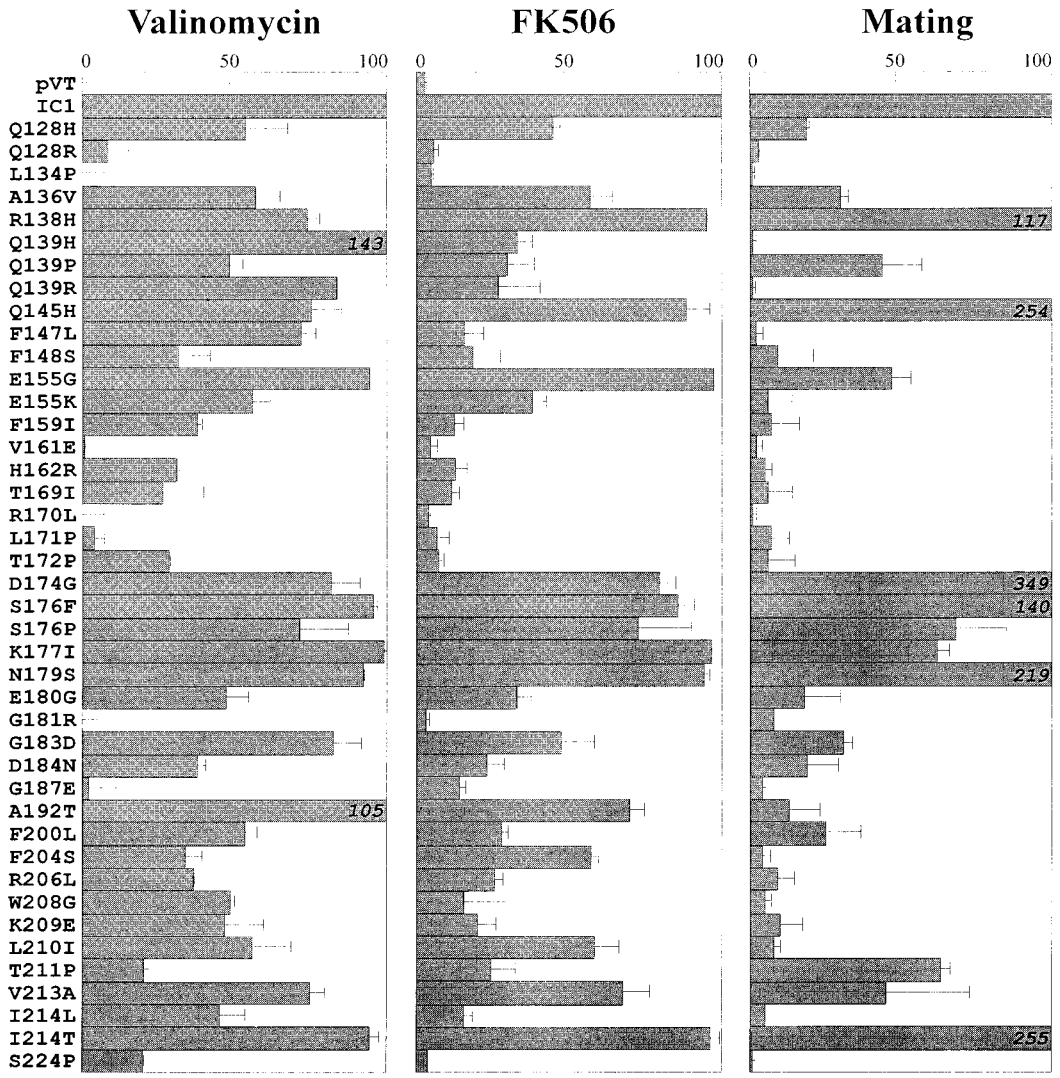

FIGURE 3: Functional analysis of mutant P-gp variants. Yeast *S. cerevisiae* transformants expressing either wild-type (IC1), or individual mutants together with pVT control cells (pVT), were grown for 22 h at 30 °C in YPD medium containing either valinomycin (50 μg/mL) or FK506 (50 μg/mL), and growth was determined by measuring optical density (A_{595}). Results are presented as relative growth, expressed as a percentage of each transformant in drug-containing medium compared to growth in YPD drug-free medium for the same period. The ability of mutant P-gps to complement a null mutant at the endogenous yeast *ste6* locus was tested in a mating assay, as described in Materials and Methods. Mating efficiency was calculated as the fraction of *mdr3* JPY201 transformants (*a* cells) capable of mating to a tester stock of the opposite mating type (DC17, α cells); it is expressed as a percentage of the control value calculated for JPY201 cells expressing wild-type P-gp (WT).

formants, and representative class 1 and class 2 mutants from different regions of the protein. This pattern of staining is consistent with that previously seen for P-gp and other ABC transporters functionally expressed in yeast (*17*, *18*) and indicates plasma membrane expression of a good portion of the mutant P-gps synthesized in these cells. Together, these experiments suggest that none of the mutants generated in this study severely impede proper membrane insertion and targeting of P-gp in the yeast host in which their function was assessed.

Expression of mdr3 mutants in P. pastoris. The *P. pastoris* expression system was used to express and functionally characterize a representative subset of 11 loss of function mutants mapping to the various structural domains targeted for random mutagenesis: Q128R, Q139H, F147L, E155K, T169I, T172P, G181R, A192T, W208G, L210I, and S224P. The full length WT and mutant *mdr3* cDNAs were subcloned into the vector pHILD2 that allows insertion at the endogenous *AOX1* locus by homologous recombination. *P. pastoris* can use methanol as its sole source of carbon through high level expression of alcohol oxidase at the *AOX1* locus. Heterologous sequences introduced by homologous recombination at the *AOX1* locus can be overexpressed under conditions of methanol induction; however, this abrogates the capacity of the yeast to grow due to the loss of the alcohol oxidase gene. Approximately 10% of the *P. pastoris* transformants with WT or mutant *mdr3* cDNAs were positive for slow growth on methanol (*m*ethanol *u*tilizing *s*low or mut^s) and of these, 100% were positive for P-gp expression as detected by immunoblotting of crude lysate proteins using the P-gp specific antibody, C219 (not shown). Membrane-enriched fractions were prepared from these clones, separated by SDS−PAGE and stained with Coomassie-Blue (Figure 6A). A band of 140 kD was readily detectable in all samples which was absent in a control clone transformed with the pHILD2 vector alone. Immunoblotting of the membrane proteins with the C219 antibody (Figure 6B) confirmed that the 140 kD band seen in the WT and mutants was indeed

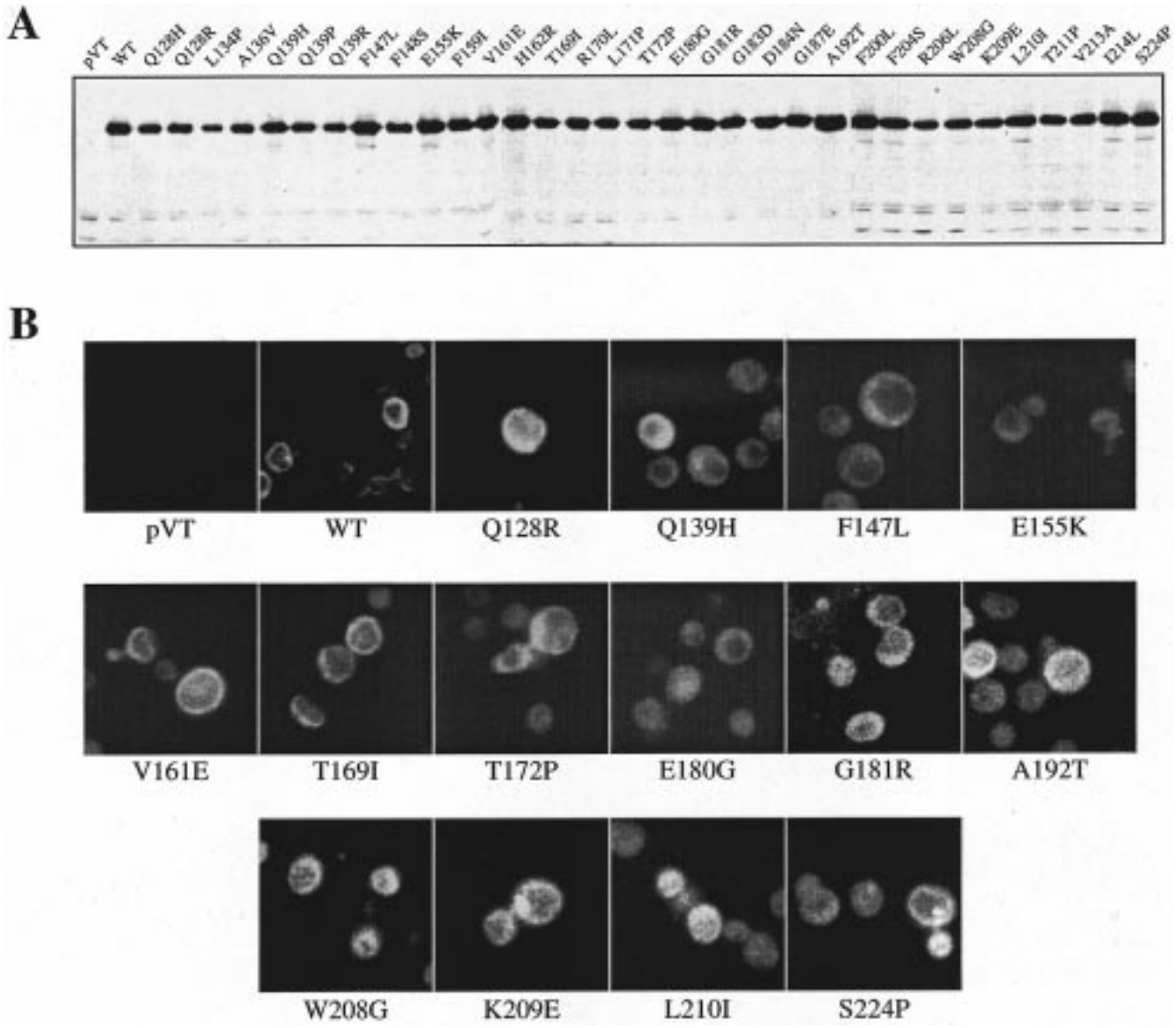

FIGURE 4: Immunodetection of wild-type and mutant P-gp variants expressed in *S. cerevisiae* yeast cells. (A) Immunoblotting of membrane enriched preparations from yeast transformants expressing individual Mdr3 variants. The mouse anti-P-glycoprotein monoclonal antibody C219 (*23*) was used to detect Mdr3 protein expression as previously described (*53*). (B) Immunofluorescence analysis of yeast cells transformed with either pVT control plasmid (pVT), wild-type *mdr3* (WT), or a representative subset of class 1 and class 2 mutants. Cells were fixed and blocked as described in Materials and Methods followed by exposure to the rabbit anti-mouse P-gp antiserum ES4 (*63*), followed by incubation with a second goat anti-rabbit antibody conjugated to Texas-red. Cells were photographed using a fluorescence microscope as described previously (*17, 18*).

P-gp. Therefore high level expression of all mutant P-gps could be achieved in the *P. pastoris* system, and none of the mutations analyzed seemed to dramatically impede proper targeting in this heterologous system.

Drug-Stimulated ATPase Activity of Mutant P-gps. P-gp expressed in *Pichia* is functional and show the characteristic ATPase activity which can be stimulated by MDR drugs or P-gp modulators such as vinblastine, valinomycin, and verapamil, respectively (*57*). Possible modulatory effects of the various mutations on the drug-stimulatable ATPase activity of the P-gps was measured after enrichment of P-gp from *P. pastoris* membranes, according to a protocol we have previously described and which is based on selective detergent extraction followed by reconstitution in *E. coli* lipids (*57*). Upon addition of 100 μM verapamil (VRP) to the P-gp enriched proteoliposomes, ATP hydrolysis by WT *mdr3* was stimulated to a V_{max} of 78 nmol/min/mg. This represents a stimulation of 2.8-fold for VRP above background levels detected in the absence of drug. Conversely, the basal ATPase activity present in membrane fractions from the pHILD2 negative control was not stimulated by the addition of VRP (0.8×) in the assay (Table 2). A similar Mdr3-specific stimulation was observed when valinomycin (100 μM, VAL) was used as a modulator, with a corresponding V_{max} of 72 nmol/min/mg or a 2.6-fold increase above background for the WT *mdr3* (data not shown).

The calculated V_{max} and K_m for the ATPase activity of each mutant was determined under conditions of VRP stimulation, and results are shown in Table 2. ATP hydrolysis was also measured under conditions of VAL stimulation, and results were very similar to those obtained with VRP. Two of the mutants displayed VRP- and VAL-stimulated ATPase activity that were similar or better than those detected in membrane extracts from WT Mdr3

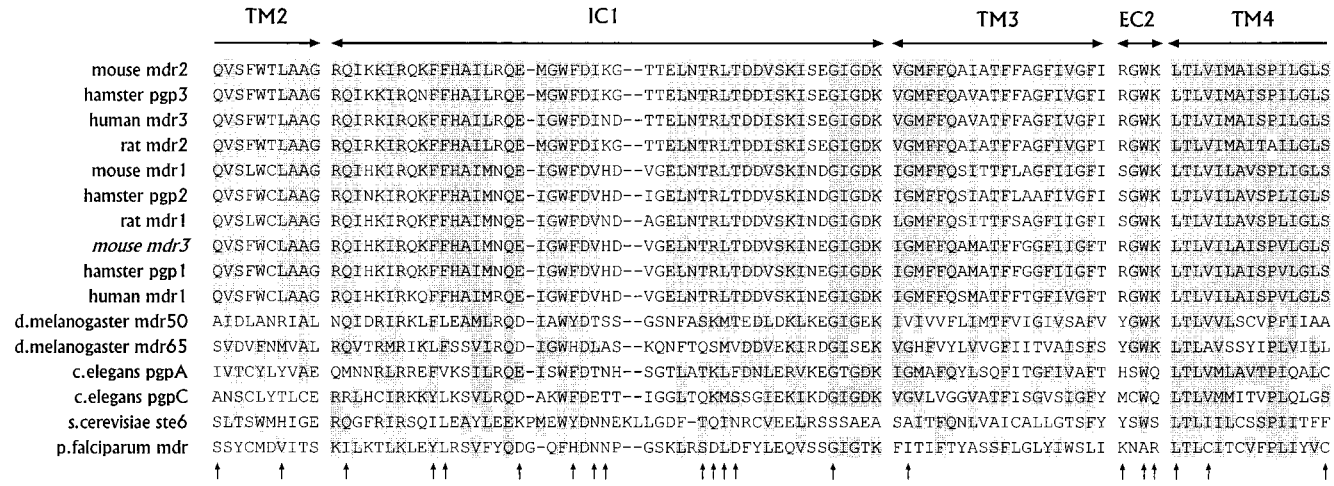

FIGURE 5: Alignment of predicted amino acid sequences from mammalian P-gps and other ABC transporters in the mutagenized region. Identical residues and conserved substitutions are shaded in gray. Arrows point to residues where mutations result in a noticeable phenotype in one or more of the assays used in our study. The sequences were obtained from Genbank and aligned using the PILEUP program of the GCG software package.

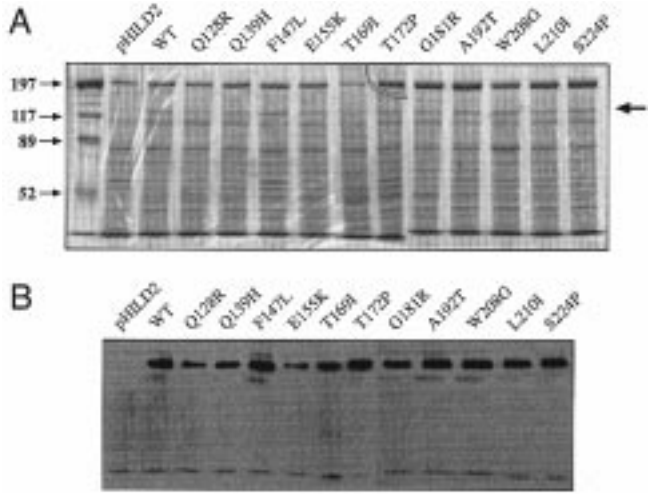

FIGURE 6: Detection of mouse Mdr3 variants in membrane preparations from *P. pastoris*. (A) Crude membrane extracts were prepared from pHIL-*mdr3 his*$^+$*mut*^{s} transformants (lanes 3−14) transformed with either wild-type *mdr3* (WT) or with various mutants (identified), and from a control clone transformed with the vector alone (pHILD2). A 10 μg amount of protein was loaded in each lane, separated by SDS-PAGE, and the gel was stained with Coomassie blue. (B) Western blot analysis of the samples shown in A using the anti-P-gp monoclonal antibody C219. The position of the molecular mass markers is indicated to the left of the gel.

expressing cells: F147L (105%, 100% of WT) and W208G (150%, 134%) (Figure 7). Two other mutants showed VRP and VAL-stimulated specific activities that were intermediate: T172P (53%, 26% of WT) and A192T (45%, 29% of WT). The remaining mutants (Q128R, Q139H, E155K, T169I, G181R, L210I, and S224P) had no significant level of ATP hydrolysis above background (pHILD2 negative control). To determine if the reduced ATPase activity in these mutants was due to a decrease in binding affinities of the NB for Mg^{2+}ATP, ATPase activity was measured in the presence of 100 μM VRP and with increasing concentrations of Mg^{2+}ATP, and velocity plots were generated. The calculated K_m for the WT Mdr3 was determined to be 0.6 mM for VRP. The K_m of the VRP stimulated ATPase activity was found to be in the same range for the mutants

Table 2: ATPase Activities of P-gp Mutants[a]

	no drug, V_{max}	V_{max}	VRP stimulation	K_M
pHILD2	0.037	0.031	0.8	ND
WT	0.028	0.078	2.8	0.6
Q128R	0.022	0.034	1.6	ND
Q139H	0.023	0.028	1.3	ND
F147L	0.039	0.081	2.0	0.8
E155K	0.033	0.034	1.0	ND
T169I	0.014	0.017	1.2	ND
T172P	0.032	0.056	1.7	0.9
G181R	0.032	0.033	1.1	ND
A192T	0.035	0.052	1.5	0.6
W208G	0.046	0.100	2.2	0.9
L210I	0.042	0.046	1.1	ND
S224P	0.032	0.032	1.0	ND

[a] Summary of kinetic analysis performed on a representative sample of mutants. The units for V_{max} are given as μmol/min/mg total protein. Drug stimulation is represented as the maximal fold stimulation. Values for K_m are given as mM concentration.

F147L, T172P, A192T, and W208G, which was between 0.6 and 1.0 mM and similar to the WT isoform. K_m values could not be determined for the remaining mutants (Q128R, Q139H, E155K, T169I, G181R, L210I, S224P) which displayed no significant drug-stimulated ATP hydrolysis above background. Altogether, these experiments indicate that all but two mutations in the protein domains studied cause either a partial or complete loss of drug-stimulated ATPase of the protein. This suggests that the molecular basis for the different phenotypes noted in intact cells for our mutants is in most cases linked to an alteration in the drug-induced ATPase activity.

DISCUSSION

A large body of published structure/function studies on P-gp have clearly established that the TM regions of this protein play an important role in substrate recognition, while the predicted NB sites are responsible for ATP binding and hydrolysis (*2*). It has also been clearly demonstrated that interaction of P-gp with certain of its drug substrates or inhibitors, presumably by TM domains within the membrane, induces ATP hydrolysis by the intracellular NB sites of the

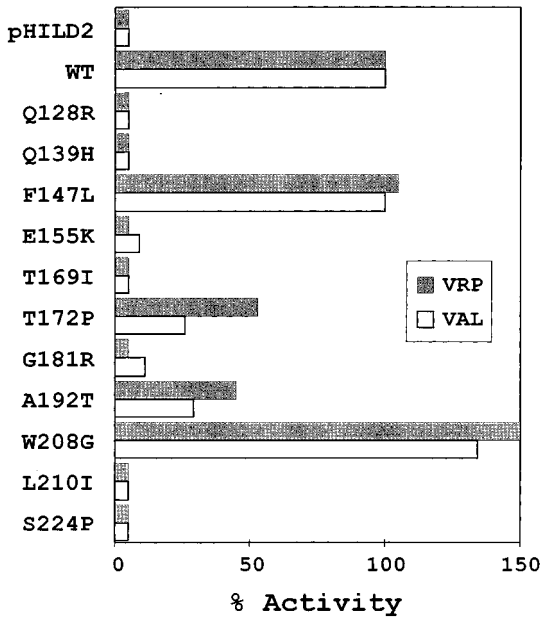

FIGURE 7: Drug-stimulated ATPase activity of P-gp mutants expressed in *P. pastoris*. Detergent extracts enriched for the various P-gp variants were prepared and reconstituted in *E. coli* lipids as described in Materials and Methods. ATPase activity was measured in these extracts under conditions of stimulation by verapamil (VRP) and valinomycin (VAL). The maximum velocity of the measured ATPase activity (V_{max}) was calculated for each clone and is expressed as a percentage of that measured in control membranes expressing the wild-type (WT) Mdr3 protein. No significant VRP or VAL stimulatable ATPase activity was noted in control membrane extracts from a clone transformed with the empty plasmid vector (pHILD2).

protein (unique drug inducible ATPase activity). Indeed, mutations at certain positions in the TM regions and the NB sites alter both substrate specificity of the protein and inducible ATPase activity (*30, 58*). The precise mechanism of signaling from the TM domains, upon drug binding, to the NB sites for induction of ATP hydrolysis remains unknown. The mechanism by which ATP hydrolysis at NB sites causes a structural change in the protein, presumably at the TM domains, to cause efflux of substrates is also unknown. We would like to gain insight into these mechanisms, and in particular, clarify a possible role of highly conserved intracellular loops and flanking TM domains in this process. As a first step, we wanted to create a mutation map of the IC1 region, including the identification of residues important for function and the preliminary characterization of cellular phenotypes biochemical alterations associated with mutations at these positions.

For this, we have used a random mutagenesis approach coupled to reinsertion of mutated segments in the full length cDNA by homologous recombination in the yeast *S. cerevisiae* followed by functional analysis in this host. Although several experimental protocols have been described for random mutagenesis such as chemical mutagenesis (*59*) and the use of mutator strains of *E. coli* (*60*), we opted for a PCR-based approach (*50*) because it is rapid, it allows the targeting of a specific sub-fragment of the cDNA, and it is largely unbiased when four reactions with each rate-limiting nucleotide are prepared. Subsequently, the mutated fragments were reintroduced as pools into the full length *mdr3* cDNA by homologous recombination in yeast, and the resulting mutants were assessed for biological activity by their ability to confer cellular resistance to the antifungal MDR drugs, FK506 and valinomycin, and also by their capacity to complement the endogenous yeast ABC transporter STE6 and restore mating in a sterile (Δste6) host. These mutagenesis and screening procedures allowed the identification of 36 positions, in the possible 106 residue segment of TM2/IC1/TM3/EC2/TM4 tested, at which mutations caused altered function. One question that emerges from these results is the following: have all mutation sensitive residues been identified in this screen or are there others that have gone undetected either because of the protocol used or because of the limited number (*782*) of mutants screened? Although it is probable that the introduction of nonconservative substitutions at certain residues resulting in partial or complete loss of function may not have been systematically tested in our mutagenesis protocol, what we were most interested in was the identification of truly "mutation sensitive" residues whose chemical properties (size, charge, hydrogen bonding, etc.) are important for P-gp function and do not tolerate any mutation without a noticeable loss of function. On the basis of the following observations, we feel that most of these residues were identified in our screen. First, nucleotide sequencing in pilot experiments indicated that conditions selected for PCR mutagenesis yielded at least one nucleotide change per mutant molecule in 80% of the cases. Second, sequencing of random "mutant" clones showing wild-type activity also identified single nucleotide substitutions in approximately 80% of the cases. Third, multiple independent mutations resulting in partial or complete loss of function were identified at what appears to be certain key residues (e.g. Q139, T169, L171, T172, G183). Fourth, no mutations with functional consequences were identified in the few short amino acid segments (central portions of IC1 and TM3) that are not conserved among members of the P-gp family (or other ABC transporters) and are therefore unlikely to play a key role in common aspects of P-gp function (Figure 5). Fifth, most of the positions identified as "mutation sensitive" residues in our screen were generally highly conserved in the P-gp and ABC transporters family (Figure 5). For these reasons, we feel that our mutagenesis protocol has revealed a good number, albeit not all mutation sensitive residues in the protein segment under investigation.

With respect to the aspects of P-gp function analyzed in our screen, mutants with altered function could be loosely arranged into two major groups. The first group showed a partial or complete overall loss of function, with reduction in cellular resistance to both FK506 and valinomycin and also significant reduction in *a*-factor transport (mating) (e.g. L134, H162, T172, G181, G187, S224). Although mutants with such a phenotype were identified in all segments analyzed (TM2, IC1, TM3, EC2, TM4), we noted a cluster of four consecutive residues at position 169−172 (TRLT) in the central portion of IC1 in which mutations caused a severe overall loss of function. The four mutations detected at these positions were nonconservative and involved elimination of a charged side chain (R170L), introduction of either a bulkier side chain (T169I) or of a helix breaker (L171P, T172P). Computer analysis of these substitutions using the program "nnpredict" show that the majority of the substitutions would indeed result in local changes in secondary structure. Structural predictions of IC1 are not overly

informative and suggest that the N-terminal half of the loop is predominantly folded in a helical coil with the remainder of the loop randomly coiled. However, these four residues are perfectly conserved in all P-gps sequenced to date (Figure 5). The mechanistic basis for the overall reduction of activity observed in these mutants could involve nonspecific effects on protein function such as poor targeting to or inappropriate folding of the protein in the membrane as previously noted for mutations at certain glycine residues in this region (*38*). However, results of immunoblotting of the membrane fraction (Figure 4A) and indirect immunofluorescence in intact cells (Figure 4B) suggest that this is not the case and that these proteins are properly targeted to the membrane fraction of the yeast host used in this study. Alternatively, such mutations may reduce the overall activity of the protein by affecting its basal or inducible ATPase activity, or possibly uncoupling signal transduction from the membrane to the ATP binding sites (see below).

The second group of mutants identified in our screen had quite a distinct phenotype from the first group. Mutants from this group did not show an overall decrease in activity toward all substrates tested. Instead, the mutation caused preferential loss of function for only one or two of the three substrates tested. The most extreme examples of such mutations were Q139H, Q139R, F147L, and A192T that retained close to wild-type activity against one or more substrates but showed complete loss of function toward another one. In mutants with such a phenotype, resistance to FK506 and valinomycin seemed to segregate from complementation of mating. As shown in Figure 2B, although such mutations were found throughout the segment analyzed, a clustering of such residues was noted within the short extracellular loop separating TM3 and TM4, and in the adjacent portion of TM4 near the extracellular space. Mutations that drastically affect resistance and/or transport of one group of substrates without affecting resistance to another suggest that the residues involved may form part of a binding site, or may be indirectly involved, through TM helices packing in the membrane, in the formation of a transport path for these substrates. Mutations altering substrate specificity in a similar manner have been previously identified in the predicted TM domains of P-gp (*31*−*34*), and of other ABC transporters such as CFTR (*61*). Although epitope mapping of proteolytic peptides photolabeled with drug analogues position part of a drug binding site further C-terminal and near TM6, the clustering of such mutations in the very short EC2 and the tip of TM4 suggest that this portion of the protein may either form part of a binding site for substrates, or may be essential for protein folding of TM helices packing in the membrane for the formation of such a site. Previous studies by our group have shown that EC2 is extremely sensitive to mutations, as insertion of 11 amino acid epitope tags in this segment inactivates the protein (*24*, *25*). In addition, studies by Loo and Clarke showed that single cysteine residues inserted in this loop in a cysteineless backbone (positions 209, 211, 215 of human MDR1) produced active proteins but the single cysteines were not accessible to a water soluble maleimide reagent (*26*). Together, these results suggest that the EC2 loop is a part of a very compact structure that is not accessible to the surface of the cells, but that is very important for the formation of a drug binding site or a transport path. Interestingly, the mutation sensitive EC2 loop and adjacent portion of TM4, including the GWKLTL sequence, have been extremely conserved in the evolution of not only the P-gp family, but also of other more distant ABC transporters such as *S. cerevisiae*, *P. falciparum*, and *C. elegans* homologues (Figure 5), in particular the LTL sequence. Therefore, our mutagenesis analyses indicate that this short protein segment plays a key structural or functional role in a common aspect of transport by these distantly related proteins. The clustering of mutations affecting substrate specificity in both EC2 and the immediately adjacent portion of TM4 is similar to that seen in the corresponding portion of TM11 and EC6 in the C-terminal portion of the protein. Photoaffinity labeling experiments have suggested that TM11 maps near a major drug binding site, and we have observed, in systematic alanine scanning experiments (*62*), a clustering of mutation sensitive residues affecting substrate specificity in the distal portion of TM11 near EC6. Together, these results suggest that EC2/TM4 and the TM11/EC6 regions may play an important role in helix packing for the formation of a transport site. Such a proposition is currently being tested in photolabeling experiments in cysteine-less mutants bearing single cysteine insertions at these sites.

The molecular basis for the observed loss of function was characterized further in a subset of 11 mutants representative of the phenotypes and structural domains of P-gp analyzed. This group consisted of mutants in TM2 (Q128R), IC1 (Q139H, F147L, E155K, T169I, T172P, G181R), TM3 (A192T), EC2 (W208G), and TM4 (L210I, S224P). Mutants showing either complete loss of function in all three assays (e.g. Q128R, G181R) or retaining near wild-type activity for at least one of the substrates tested (e.g. Q139H, F147L) were included in this study. The ATPase activity of these mutants was studied after expression in the yeast *Pichia pastoris*. We have recently described a protocol for the high level expression of P-gp in the membrane fraction of *P. pastoris*, followed by detergent extraction and reconstitution in *E. coli* lipids (*57*). We showed that P-gp is fully functional in membrane extracts from this yeast with respect to drug binding characteristics and drug-stimulatable ATPase activity (K_m for Mg^{2+} ATP 0.4 mM, V_{max} = 0.209 μmol/mg/min). All mutants could be stably expressed in the membrane fractions of *P. pastoris* (Figure 6), suggesting that none of the mutations drastically affected protein stability or targeting in this yeast. A partial (*2*) or complete loss (*7*) of drug-inducible ATPase activity was noted in 9 of the 11 mutants analyzed (Table 2), therefore suggesting that most mutations affect the ATPase activity of the protein. Mutants that showed partial or complete loss of ATPase activity were identified in IC loops, EC loops, and TM domains and could also be found in the two large phenotypic groups identified in vivo in intact cells. The observation that mutations in the various structural domains analyzed were similarly expressed as partial or complete loss of drug-inducible ATPase activity suggests that TM domains (drug binding), IC and EC loops, and NBDs (ATP hydrolysis) all participate in signal transduction from TM domains (drug binding) to the NB sites (ATPase activity). The observed loss of ATPase activity in individual mutants in TM domains or EC and IC loops has previously been observed in other series of mutants in some of these regions (*30*, *41*, *58*). This suggests that the structural domains analyzed by random mutagenesis are

structurally interdependent and catalytically tightly coupled and do not function as modular units within the intact protein.

The noted wild-type levels of ATPase activity in the F147L (IC1) and W208G (EC2) mutants with respect to K_m and V_{max} are intriguing in view of the loss of function of these mutants with respect to FK506 resistance and *ste6* complementation (Figure 3). One possible explanation is that these mutants are intrinsically active with respect to transport but are not properly folded, targeted, or processed in the yeast host used for analysis. We think this possibility is unlikely in view of the near wild-type level of valinomycin resistance expressed by these mutants, and by the immunofluorescence data in Figure 4 showing a staining pattern similar to wild-type Mdr3. Although highly speculative, another possibility is that these mutations may alter an effector signal from the NB sites upon ATP hydrolysis to the TM domains to affect drug transport. This possibility is currently being tested in additional mutants at these positions.

ACKNOWLEDGMENT

We would like to thank Martine Brault, Dr. Lucille Beaudet, and Dr. Ina L. Urbatsch for helpful discussions and technical assistance during this work.

REFERENCES

1. Raymond, M., Gros, P., Whiteway, M., and Thomas, D. Y. (1992) *Science 256*, 232−4.
2. Shustik, C., Dalton, W., and Gros, P. (1995) *Mol. Aspects Med. 16*, 1−78.
3. Hanna, M., and Gros, P. (1996) in *Multidrug Resistance in Cancer Cells: Molecular, Biochemical, Physiological and Biological Aspects* (Gupta, S., and Tsuruo, T., Eds.) pp 5−28, John Wiley and Sons, New York.
4. Ruetz, S., and Gros, P. (1994) *Cell 77*, 1071−81.
5. Schinkel, A. H., Smit, J. J., van Tellingen, O., Beijnen, J. H., Wagenaar, E., van Deemter, L., Mol, C. A., van der Valk, M. A., Robanus-Maandag, E. C., te Riele, H. P. et al. (1994) *Cell 77*, 491−502.
6. Vanhelvoort, A., Smith, A. J., Sprong, H., Fritzsche, I., Schinkel, A. H., Borst, P., and Vanmeer, G. (1996) *Cell 87*, 507−517.
7. Kuchler, K., Sterne, R. E., and Thorner, J. (1989) *EMBO. J 8*, 3973−84.
8. Foote, S. J., Thompson, J. K., Cowman, A. F., and Kemp, D. J. (1989) *Cell 57*, 921−30.
9. Cole, S. P., Bhardwaj, G., Gerlach, J. H., Mackie, J. E., Grant, C. E., Almquist, K. C., Stewart, A. J., Kurz, E. U., Duncan, A. M., and Deeley, R. G. (1992) *Science 258*, 1650−4.
10. Shen, H. X., Paul, S., Breuninger, L. M., Ciaccio, P. J., Laing, N. M., Helt, M., Tew, K. D., and Kruh, G. D. (1996) *Biochemistry 35*, 5719−5725.
11. Deverson, E. V., Gow, I. R., Coadwell, W. J., Monaco, J. J., Butcher, G. W., and Howard, J. C. (1990) *Nature 348*, 738−41.
12. Monaco, J. J., Cho, S., and Attaya, M. (1990) *Science 250*, 1723−6.
13. Spies, T., Cerundolo, V., Colonna, M., Cresswell, P., Townsend, A., and DeMars, R. (1992) *Nature 355*, 644−6.
14. Trowsdale, J., Hanson, I., Mockridge, I., Beck, S., Townsend, A., and Kelly, A. (1990) *Nature 348*, 741−4.
15. Riordan, J. R., Rommens, J. M., Kerem, B., Alon, N., Rozmahel, R., Grzelczak, Z., Zielenski, J., Lok, S., Plavsic, N., Chou, J. L. et al. (1989) *Science 245*, 1066−73.
16. van Doorninck, J. H., French, P. J., Verbeek, E., Peters, R. H., Morreau, H., Bijman, J., and Scholte, B. J. (1995) *EMBO J. 14*, 4403−11.
17. Ruetz, S., Brault, M., Kast, C., Hemenway, C., Heitman, J., Grant, C. E., Cole, S. P., Deeley, R. G., and Gros, P. (1996) *J. Biol. Chem. 271*, 4154−60.
18. Ruetz, S., Delling, U., Brault, M., Schurr, E., and Gros, P. (1996) *Proc. Natl. Acad. Sci. U.S.A. 93*, 9942−7.
19. Volkman, S. K., Cowman, A. F., and Wirth, D. F. (1995) *Proc. Natl. Acad. Sci. U.S.A. 92*, 8921−8925.
20. Gros, P., Croop, J., and Housman, D. (1986) *Cell 47*, 371−80.
21. Chen, C. J., Chin, J. E., Ueda, K., Clark, D. P., Pastan, I., Gottesman, M. M., and Roninson, I. B. (1986) *Cell 47*, 381−9.
22. Yoshimura, A., Kuwazuru, Y., Sumizawa, T., Ichikawa, M., Ikeda, S., Uda, T., and Akiyama, S. (1989) *J. Biol. Chem. 264*, 16282−91.
23. Kartner, N., Evernden-Porelle, D., Bradley, G., and Ling, V. (1985) *Nature 316*, 820−3.
24. Kast, C., Canfield, V., Levenson, R., and Gros, P. (1996) *J. Biol. Chem. 271*, 9240−9248.
25. Kast, C., Canfield, V., Levenson, R., and Gros, P. (1995) *Biochemistry 34*, 4402−11.
26. Loo, T. W., and Clarke, D. M. (1995) *J. Biol. Chem. 270*, 843−8.
27. Raviv, Y., Pollard, H. B., Bruggemann, E. P., Pastan, I., and Gottesman, M. M. (1990) *J. Biol. Chem. 265*, 3975−80.
28. Greenberger, L. M. (1993) *J. Biol. Chem. 268*, 11417−25.
29. Devine, S. E., Ling, V., and Melera, P. W. (1992) *Proc. Natl. Acad. Sci. U.S.A. 89*, 4564−8.
30. Loo, T. W., and Clarke, D. M. (1994) *Biochemistry 33*, 14049−57.
31. Loo, T. W., and Clarke, D. M. (1993) *J. Biol. Chem. 268*, 3143−9.
32. Loo, T. W., and Clarke, D. M. (1993) *J. Biol. Chem. 268*, 19965−72.
33. Gros, P., Dhir, R., Croop, J., and Talbot, F. (1991) *Proc. Natl. Acad. Sci. U.S.A. 88*, 7289−93.
34. Dhir, R., Grizzuti, K., Kajiji, S., and Gros, P. (1993) *Biochemistry 32*, 9492−9.
35. Loo, T. W., and Clarke, D. M. (1995) *J. Biol. Chem. 270*, 22957−61.
36. Homolya, L., Hollo, Z., Germann, U. A., Pastan, I., Gottesman, M. M., and Sarkadi, B. (1993) *J. Biol. Chem. 268*, 21493−6.
37. Rao, U. S., and Scarborough, G. A. (1994) *Mol. Pharmacol. 45*, 773−6.
38. Loo, T. W., and Clarke, D. M. (1994) *J. Biol. Chem. 269*, 7243−8.
39. Choi, K. H., Chen, C. J., Kriegler, M., and Roninson, I. B. (1988) *Cell 53*, 519−29.
40. Safa, A. R., Stern, R. K., Choi, K., Agresti, M., Tamai, I., Mehta, N. D., and Roninson, I. B. (1990) *Proc. Natl. Acad. Sci. U.S.A. 87*, 7225−9.
41. Rao, U. S. (1995) *J. Biol. Chem. 270*, 6686−90.
42. Beaudet, L., and Gros, P. (1995) *J. Biol. Chem. 270*, 17159−70.
43. Muller, M., Bakos, E., Welker, E., Varadi, A., Germann, U. A., Gottesman, M. M., Morse, B. S., Roninson, I. B., and Sarkadi, B. (1996) *J. Biol. Chem. 271*, 1877−83.
44. Momburg, F., Armandola, E. A., Post, M., and Hammerling, G. J. (1996) *J. Immunol. 156*, 1756−1763.
45. Currier, S. J., Kane, S. E., Willingham, M. C., Cardarelli, C. O., Pastan, I., and Gottesman, M. M. (1992) *J. Biol. Chem. 267*, 25153−9.
46. Cotten, J. F., Ostedgaard, L. S., Carson, M. R., and Welsh, M. J. (1996) *J. Biol. Chem. 271*, 21279−21284.
47. Seibert, F. S., Linsdell, P., Loo, T. W., Hanrahan, J. W., Clarke, D. M., and Riordan, J. R. (1996) *J. Biol. Chem. 271*, 15139−45.
48. Devault, A., and Gros, P. (1990) *Mol. Cell Biol. 10*, 1652−63.
49. Ruetz, S., and Gros, P. (1994) *J. Biol. Chem. 269*, 12277−84.
50. Spee, J. H., de Vos, W. M., and Kuipers, O. P. (1993) *Nucleic Acids Res. 21*, 777−8.

51. Holton, T. A., and Graham, M. W. (1991) *Nucleic Acids Res. 19*, 1156.
52. Ishioka, C., Frebourg, T., Yan, Y. X., Vidal, M., Friend, S. H., Schmidt, S., and Iggo, R. (1993) *Nature Genet. 5*, 124−9.
53. Raymond, M., Ruetz, S., Thomas, D. Y., and Gros, P. (1994) *Mol. Cell. Biol. 14*, 277−86.
54. Perlin, D. S., Harris, S. L., Seto-Young, D., and Haber, J. E. (1989) *J. Biol. Chem. 264*, 21857−64.
55. Van Veldhoven, P. P., and Mannaerts, G. P. (1987) *Anal. Biochem. 161*, 45−8.
56. Kuchler, K., and Thorner, J. (1992) *Proc. Natl. Acad. Sci. U.S.A. 89*, 2302−6.
57. Beaudet, L., Urbatsch, I. L., and Gros, P. (1997) *Methods Enzymol*., in press.
58. Loo, T. W., and Clarke, D. M. (1996) *J. Biol. Chem. 271*, 15414−9.
59. Myers, R. M., Lerman, L. S., and Maniatis, T. (1985) *Science 229*, 242−7.
60. Schaaper, R. M. (1988) *Proc. Natl. Acad. Sci. U.S.A. 85*, 8126−30.
61. Anderson, M. P., Gregory, R. J., Thompson, S., Souza, D. W., Paul, S., Mulligan, R. C., Smith, A. E., and Welsh, M. J. (1991) *Science 253*, 202−5.
62. Hanna, M., Brault, M., Kwan, T., Kast, C., and Gros, P. (1996) *Biochemistry 35*, 3625−35.
63. Schurr, E., Raymond, M., Bell, J. C., and Gros, P. (1989) *Cancer Res 49*, 2729−33.

BI972680X